JOC*Article*

Energy Profiles for Ketene Cyclizations. Interconversion of 1,3-Oxazin-6-ones, Mesoionic 1,3-Oxazinium Olates and Acylketenes, Imidoylketenes, Oxoketenimines, and Cyclization Products

Holger Bornemann and Curt Wentrup*

Chemistry Building, School of Molecular and Microbial Sciences, The University of Queensland, Brisbane, Qld 4072, Australia

wentrup@uq.edu.au

Received March 6, 2005

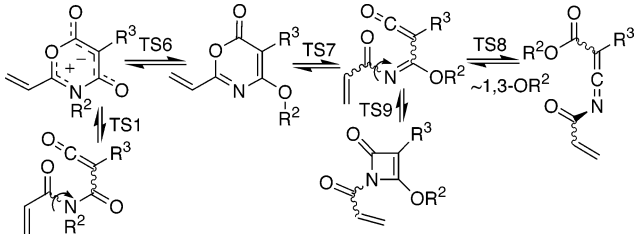

The energy surface connecting oxazinium olates **9**, several possible conformers of ketenes **10** and **11**, and the final cyclization products **12**, **13** and **14**, as well as the isomeric 1,3-oxazine-6-ones **15**, ring opening of the latter to *N*-acylimidoylketenes **16**, and subsequent rearrangement of **16** to oxoketenimines **17**, azetinones **18**, and the cyclization products **19** and **20** are evaluated computationally at the B3LYP/6-31G* and B3LYP/6-311+G*//B3LYP/6-31G* levels. The cyclizations of ketenes to oxazinium olates **9** and oxazines **15** have the characteristics of pseudopericyclic reactions. Plots of the energy vs internal reaction coordinate for the cyclization of transoid acylketenes such as **10** to **9** (via **TS1**) and **16** to **15** (via **TS7**) feature two inflection points and indicate that the part of the energy surface above the lower inflection points describe internal rotation of the acyl function in the ketene moiety, and the part below this point describes the cyclization of the cisoid ketene to the planar mesoionic oxazinium olate **9** or oxazinone **15**. The 1,3-shifts of the OR group that interconvert ketenes **16** and ketenimines **17** via four-membered cyclic transition states **TS8** behave similarly, the first portion (from the ketenimine side) of the activation barrier being due largely to internal rotation of substituents, and the top part being due to the 1,3-shift proper.

Introduction

We have recently reported the valence isomerization of mesoionic oxazinium olates **1** to 3-azabicyclo[3.1.1]-heptanetriones **2** via transient acylketenes (eq 1).[1] Pyridopyrimidinium olates **3** undergo analogous valence isomerization to acyl- or imidoylketenes **4**, which takes place in solution at or slightly above room temperature (eq 2).[2] Although the transient ketenes **4** could not be observed directly, the calculated activation barrier for the ring opening, **3** → **4**, was as low as 20 kcal/mol in one case.[2a] The formally nonmesoionic pyridopyrimidinones **5** undergo reversible ring opening to imidoylketenes **6** under conditions of flash vacuum thermolysis (FVT) (eq 2).[2,3] In addition, five-membered heterocyclic mesoionic compounds can undergo valence isomerization to the ring-opened ketenes, albeit sometimes with more difficulty.[4,5] The ring-opening reactions of **1**, **3**, and **5** are of considerable interest as likely examples of pseudopericyclic reactions,[6] taking place via a planar or nearly planar transition state and with very low activation barriers from the ketenes to the cyclized products. The

(1) Sheibani, H.; Bernhardt, P. V.; Wentrup, C. *J. Org. Chem.* **2005**, *70*, 5859−5861.

(2) (a) Andersen. H. G.; Mitschke, U.; Wentrup, C. *J. Chem. Soc., Perkin Trans. 2,* **2001**, 602−607. (b) Fiksdahl, A.; Plüg, C.; Wentrup, C. *J. Chem. Soc., Perkin Trans. 2* **2000**, 1841−1845.

(3) Plüg, C.; Frank, W.; Wentrup, C. *J. Chem. Soc., Perkin Trans. 2* **1999**, 1087−1093.

(4) Plüg, C.; Wallfisch, A.; Andersen, H. G.; Bernhardt, P. V.; Baker, L.-J.; Clark, G. R.; Wong, M. W.; Wentrup, C. *J. Chem. Soc., Perkin Trans. 2* **2000**, 2096−2108.

(5) (a) Pyrrolo[1,2-*a*]pyridinylium olates to (2-pyridyl)carbonylketenes: Ye, X.; Andraos, J.; Bibas, H.; Wong, M. W.; Wentrup, C. *J. Chem. Soc., Perkin Trans. 2* **2000**, 401−406. (b) Photochemical ring opening of sydnones to *N*-nitrosaminoketenes: Veedu, R. N.; Wentrup, C. Unpublished results, The University of Queensland, 2004.

(6) (a) Birney, D. M.; Wagenseller, P. E. *J. Am. Chem. Soc.* **1994**, *116*, 6262−6270. (b) Birney, D. M. *J. Org. Chem.* **1996**, *61*, 243−251.

10.1021/jo050429e CCC: $30.25
Published on Web 06/23/2005

SCHEME 1

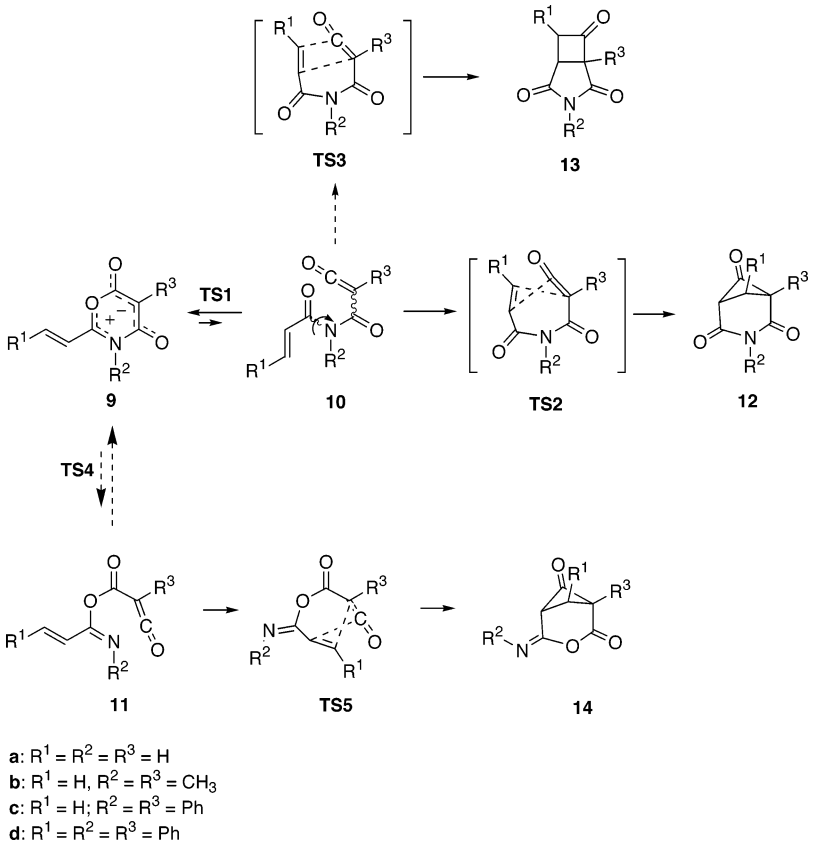

reactions are akin to the valence isomerization of α-pyrones (**7a**) (and analogously coumarins to ketenes), 1,3-oxazin-6-ones (**7b**), 1*H*-pyridin-2-ones (**7c**), and 2,4-cyclohexadienones (**7d**) to the corresponding ketenes **8a**−**d** (eq 3), which have been the subject of considerable recent experimental[7] and theoretical[6b,7c,d,8] investigation.

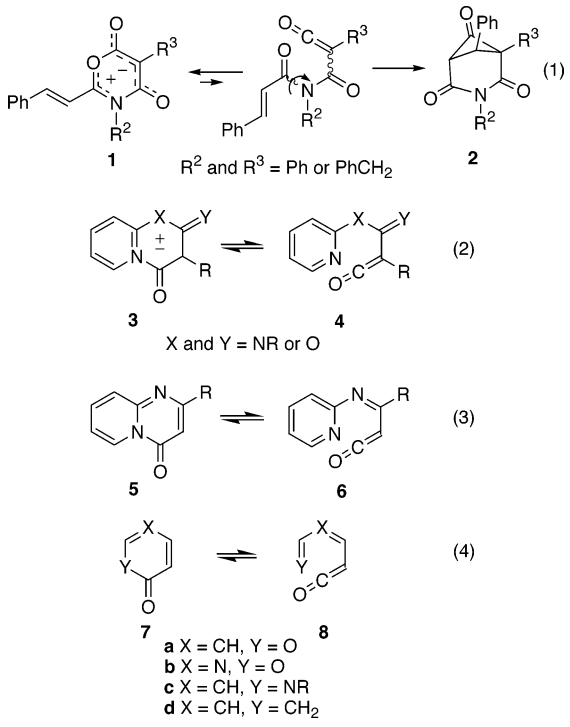

To provide a deeper understanding of the reaction paths of oxazinium olates and oxazinones, we now report a theoretical investigation of the 2-vinyl-1,3-oxazinium olates **9**, their facile ring opening to ketenes **10** and recyclization to 3-azabicyclo[3.1.1]heptanetriones **12**, rearrangement to nonmesoionic oxazinones **15**, and the isomerizations and cyclizations of the latter involving ketenes, ketenimines, and azetinones.

Results and Discussion

DFT calculations on the species shown in Scheme 1 were performed at the B3LYP/6-31G* (**a**−**d** series) and B3LYP/6-311+G*//B3LYP/6-31G* levels (**a** and **b** series) using the Gaussian 03 suite of programs.[9] The resulting energy profiles for the dimethyl (**9b**) and the triphenyl derivatives (**9d**) are shown in Figure 1. The corresponding figures for **9a** and **9c** are similar, and they are all shown in the Supporting Information (Figures S1−S4, Supporting Information). Compounds **9d** and **12d** were characterized experimentally.[1]

(7) (a) Thermal ring opening of α-pyrones and coumarins to ketenes: Wentrup, C.; Heilmeyer, W.; Kollenz, G. *Synthesis* **1994**, 1219−1248. (b) Matrix photochemical ring opening of α-pyrones to ketenes: Breda, S.; Reva, I.; Lapinski, L.; Fausto, R. *Phys. Chem. Chem. Phys.* **2004**, *6*, 929−937. Breda, S.; Reva, I.; Lapinski, L.; Fausto, R. *Photochem. Photobiol.*. **2004**, *162*, 139−151. (c) *N*-Acylimidoylketene to 1,3-oxazin-6-one: Alajarin, M.; Sanchez-Andrada, P.; Cossio, F. P.; Arrieta, A. *J. Org. Chem.* **2001**, *66*, 8370−8477. (d) *N*-Acylvinylketenimine cyclizations: Alajarín, M.; Sánchez-Andrada, P.; Vidal, A.; Tovar, F. *J. Org. Chem.* **2005**, *70*, 1340−1349.

(8) (a) Oxovinylketenes to α-pyrones and analogous hetero-1,2,4,6-heptatetraene cyclizations: Rodriguez-Otero, J.; Cabaleiro-Lago, E. M. *Chem. Eur. J.* **2003**, *9*, 1837−1843. (b) Zora, M. *J. Org. Chem.***2004**, *69*, 1940−1947.

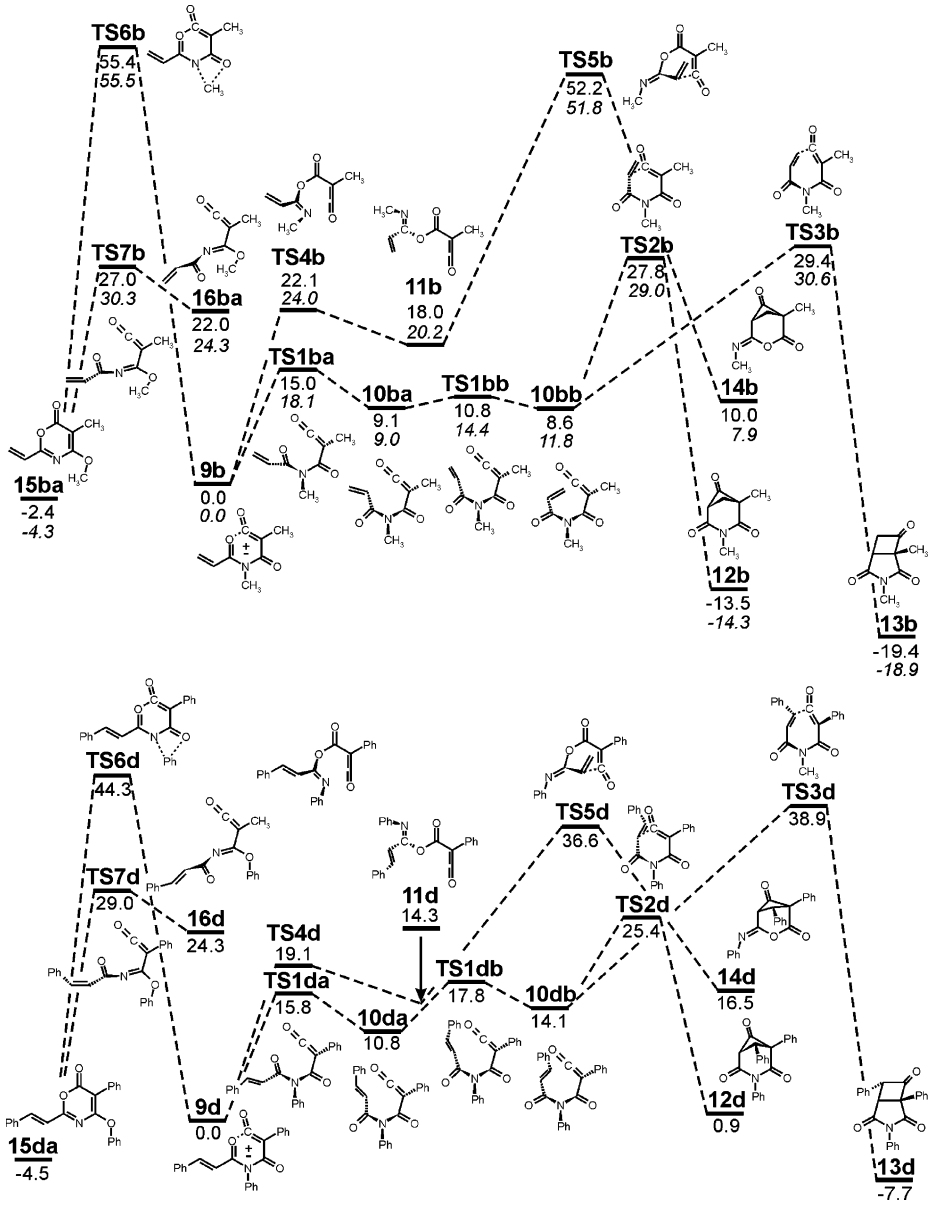

FIGURE 1. (Top): energy profile for oxazinium olate **9b** and its isomers (roman numbers, B3LYP/6-311+G*//B3LYP/6-31G*; italic numbers, B3LYP/6-31G* energies (kcal/mol). (Bottom): energy profile for oxazinium olate **9d** and its isomers at the B3LYP/6-31G* level (kcal/mol).

The absolute and relative energies, zero-point energy corrections, and imaginary frequencies for transition states are listed in Tables S1−S6 (Supporting Information). Transition states for the **a** and **b** series were confirmed using IRC calculations. This level of calculation has been shown previously to be reliable for structures of the types considered here.[2,4,5a,6,7c,d,8]

Oxazinium Olates. The calculated gas-phase structures ($\epsilon = 0$) of oxazinium olates **9** are highly distorted in the direction the ring-opened ketenes **10**, most dramatically in the case of the parent compound **9a** (Chart 1). It is apparent that the trisubstituted compounds **9b**−**d** are better able to stabilize the positive charge in the cyclic, mesoionic structures, thus making them less ketene-like. All of the compounds have calculated IR absorptions at very high wavenumbers, 2178−1880 cm^{-1} (unscaled; Figures S1 and S2, Supporting Information), which is more in line with ketenes than carbonyl groups, again especially for the parent compound **9a** (2178 cm^{-1}). These gas-phase structures of **9** are slightly less stable than the nonmesoionic oxazinone isomers **15** (see Figure 1 and Figures S1−S4, Supporting Information). However,

(9) Frisch, M. J.; Trucks, G. W.; Schlegel, H. B.; Scuseria, G. E.; Robb, M. A.; Cheeseman, J. R.; Montgomery, J. A., Jr.; Vreven, T.; Kudin, K. N.; Burant, J. C.; Millam, J. M.; Iyengar, S. S.; Tomasi, J.; Barone, V.; Mennucci, B.; Cossi, M.; Scalmani, G.; Rega, N.; Petersson, G. A.; Nakatsuji, H.; Hada, M.; Ehara, M.; Toyota, K.; Fukuda, R.; Hasegawa, J.; Ishida, M.; Nakajima, T.; Honda, Y.; Kitao, O.; Nakai, H.; Klene, M.; Li, X.; Knox, J. E.; Hratchian, H. P.; Cross, J. B.; Bakken, V.; Adamo, C.; Jaramillo, J.; Gomperts, R.; Stratmann, R. E.; Yazyev, O.; Austin, A. J.; Cammi, R.; Pomelli, C.; Ochterski, J. W.; Ayala, P. Y.; Morokuma, K.; Voth, G. A.; Salvador, P.; Dannenberg, J. J.; Zakrzewski, V. G.; Dapprich, S.; Daniels, A. D.; Strain, M. C.; Farkas, O.; Malick, D. K.; Rabuck, A. D.; Raghavachari, K.; Foresman, J. B.; Ortiz, J. V.; Cui, Q.; Baboul, A. G.; Clifford, S.; Cioslowski, J.; Stefanov, B. B.; Liu, G.; Liashenko, A.; Piskorz, P.; Komaromi, I.; Martin, R. L.; Fox, D. J.; Keith, T.; Al-Laham, M. A.; Peng, C. Y.; Nanayakkara, A.; Challacombe, M.; Gill, P. M. W.; Johnson, B.; Chen, W.; Wong, M. W.; Gonzalez, C.; Pople, J. A. *Gaussian 03*, Revision B.05; Gaussian, Inc., Wallingford, CT, 2004.

CHART 1. Calculated Structures of Oxazinium Olates 9 in the Gas Phase ($\epsilon = 0$) and in Solution ($\epsilon = 40$)

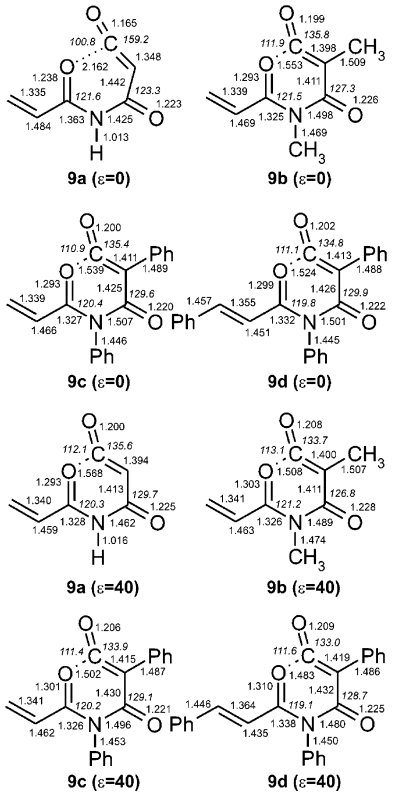

we have shown previously that it is necessary to simulate a strong dipolar field, typically with dielectric constants $\epsilon = 10-40$ in order to get good calculated structures and IR spectra of such highly polar compounds.[2] Application of a dipolar field with $\epsilon = 40$ stabilizes the mesoionic compounds **9** by a few kcal/mol, so that they now become slightly more stable than the tautomeric nonmesoionic oxazinones **15** (Scheme 2 and Tables S1−S6, Supporting Information). Moreover, the characteristic IR absorptions of the carbonyl groups in **9** move to lower frequencies, although they are still very high (1915−1838 cm^{-1} (unscaled; Figures S5 and S6, Supporting Information). The structures are now clearly cyclic, distorted oxazinium olates with long O−CO bonds (1.48−1.57 A) and acute O−CO angles (112−113°) (Chart 1). The N−CO (exocyclic) bonds are also long (1.46−1.50 A), and the N−CO angles are acute (115−117°). The effect is the strongest for the O−CO link, and thus it is here that ring opening is expected, leading to ketene **10** rather than **11**, in accord with the energy calculations in Figure 1 and the experimental results. The calculations reported in Figure 1 are for the gas phase ($\epsilon = 0$). In these figures, we represent **9** by structures that are intermediate between the ketene-type structures calculated for the gas phase and the mesoionic cyclic ones calculated for polar media and observed experimentally. The true calculated structures are shown in Chart 1.

It is seen in Figures 1 and S1−S4 (Supporting Information) that the energies of **TS2** and **TS3** are not very different for the reactions of ketenes **10ab**−**10cb**, but the addition of a phenyl substituent on the vinyl groups raises **TS3** very drastically, so that **TS2**, leading to products **12d**, becomes the only experimentally observed

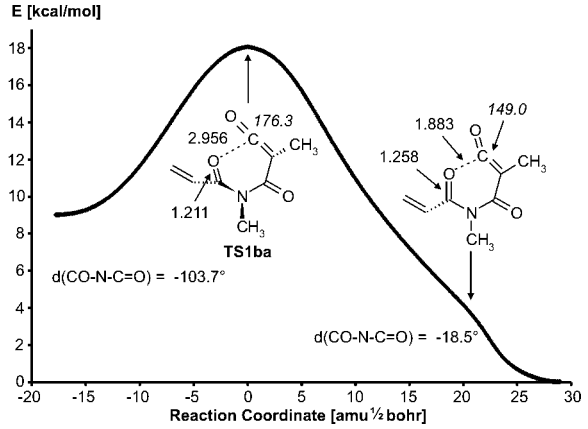

FIGURE 2. Plot of energy vs internal reaction coordinate for ketene **10b** via **TS1ba** to mesoion **9b** (B3LYP/6-31G*).

reaction[1] even though, in all cases, the nonobserved product **13** is thermodynamically more stable. Olate **9d** only has to overcome a barrier of 25 kcal/mol in order to isomerize to bicyclic product **12d**. Since the olates **9** undergo ring opening to amidylketenes **10d** and related compounds[1] with activation barriers well below 20 kcal/mol, and the ketenes are ca. 10 kcal/mol above the olates in energy, the ketenes cannot be directly observed under the reaction conditions, even though they are calculated to exist in formal equilibrium with the olates at room temperature. At equilibrium, ketene **10db** only needs a further 11 kcal/mol to cyclize to **12d** (Figure 1).

Ketene−Oxazinium Olate Interconversion. The transition states for ring opening of the oxazinium olates **9** to ketene **10** and **11**, namely **TS1** and **TS4**, are interesting. These are expected to be planar, pseudopericyclic reactions, in which the planar cisoid ketenes are not likely to be computational minima because they should undergo ring closure to the oxazinium olates with very small activation energies. At the HF/6-31G* level the planar cisoid ketene **10a** (not shown; C=O and C=C=O in s-cis arrangement for six-membered-ring formation) is a shallow minimum, 0.1 kcal/mol above the planar mesoion **9a** (the ketene conformer **10a** is 7.9 kcal/mol lower in energy than the mesoion at the HF level). At the B3LYP/6-31G* level the lowest energy stable ketene conformer of **10a** (Figure S1, Supporting Information) is found to cyclize to olate **9a** via **TS1a**, in which the C=O group of the amide moiety is nearly perpendicular to the C=C=O moiety with which it will react. This implies that, as soon as any of the ketene conformers of **10a** has rotated past the perpendicular arrangement in **TS1a**, the energy drops rapidly until the cyclic structure **9a** is reached.

A plot of the energy versus internal reaction coordinate for the dimethyl-substituted ketene **10b** from **TS1ba** (Figure 1) to the mesoion **9b** is informative. As seen in Figure 2, the graph shows a second inflection point and a steep drop in energy when the imine function is at a dihedral angle [∠(O=C)−N−C=O] of 18.5° from the planar mesoion **9b**. This inflection point is 4 kcal/mol above the mesoion (**TS1ba** is 18.1 kcal/mol above the mesoion). The structure at the inflection point resembles that of the mesoion strongly. The distance between the cyclizing atoms O3 and C4 is 1.9 Å (1.5 Å in the mesoion: Chart 1), and the C=C=O angle in the ketene

is 149° (136° in the mesoion in the gas phase, 134° in the mesoion at $\epsilon = 40$: Chart 1). While we have not actually located a transition for the *cyclization* of the planar cisoid ketene **10** to mesoion **9**, if such a TS existed, i.e., if rotation and cyclization were sufficiently uncoupled, we would expect it in the region of the inflection point. In the initial region of the IRC above the inflection point the species is the ketene undergoing internal rotation. In the final region below the inflection point the species is essentially the mesoion. Thus, by far the major part of the activation barrier is due to internal rotation. The actual cyclization process has a very low activation barrier as expected for an essentially planar, pseudopericyclic reaction. Somewhat different cases of consecutive transition states were reported by Bartsch et al.[10a] for a rotation−cyclization reaction, and by Finnerty et al.[10b] for rotation plus 1,3-shift interconverting imidoylketenes and oxoketenimines (see also the section on 1,3-shift in ketenes and ketenimines below).

A similar situation obtains for the cyclization of iminooxycarbonylketenes **11** via **TS4** to olate **9** (Figure 1). As shown in the Supporting Information (Figure S14), the dihedral angle between the imine function and the ketene in **TS4b** is ca. 123°. The energy profile is rather flat-topped around **TS4b**, corresponding to internal rotation of the imine function, which continues after **TS4b** has been reached, and the cyclization proper starts only after the TS has been passed. The energy then drops until **9a** is reached without any further intermediate being located at the DFT level. At the HF/6-31G* level it was possible to locate a planar cisoid ketene existing between **TS4a** and **9a**, but with a tiny barrier (0.3 kcal/mol) to ring closure to **9a**. The cisoid ketene is 14.8 kcal/mol above the mesoion at the HF level. These results are analogous to the situation for ketenes **6a**,**b**,**d** for which detailed calculations have demonstrated the pseudopericyclic nature of their cyclization reactions.[6b,8]

Oxazinones. Mesoions **9** could in principle tautomerize to the nonmesoionic analogue **15** (Scheme 2, Figure 1, and Figures S1−S4 (Supporting Information)). The intramolecular H-shift of **9a** would require an activation energy of ca. 33 kcal/mol, but an intermolecular H-transfer would be more likely in solution. As mentioned above, the mesoions are actually slightly more stable than the oxazinones in the presence of a strong dipolar field (simulating their own dipolar field). The isomerization of the substituted mesoions **9b**−**d** to oxazinones **15** would require 1,3-shifts of substituents from N to O. These reactions have even higher activation barriers and are not likely to occur, except possibly under FVT conditions. However, oxazinones can be synthesized in other ways and may undergo thermal ring opening to ketenes.[11] It is therefore of interest to examine a further set of isomerizations on the same energy surface emanating from the ring opening of oxazinones **15** to imidoylketenes **16** (Scheme 2 and Figures 3 and 4).

Ketene−Oxazinone Interconversion. The ring opening of oxazine **15a** to imidoylketene **16a** has a calculated barrier of ca. 30 kcal/mol (Figure 3). Compound **16a** is

SCHEME 2

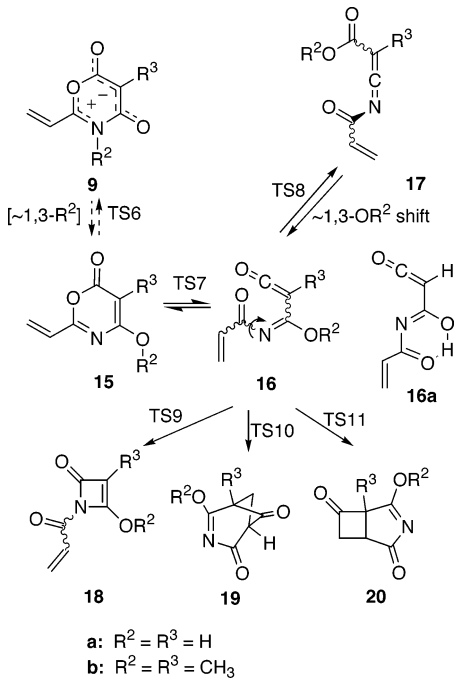

locked in a transoid conformation **16aa** (Scheme 2 and Figure 3) by an O−H−O hydrogen bond, which stabilizes the compound considerably (compare Figures 3 and 4), thereby raising the barrier toward ring closure. As in the previous cases (**TS1** and **TS4**), a planar cisoid ketene was not found at the DFT level. The transition state for the ring closure of ketene **16aa** to oxazinone **15a**, **TS7a**, has a dihedral angle of 94.5° between the ketene and carbonyl moieties. On the energy profile for rotation of the C=O group of the amide function toward a planar structure there is a clear inflection point at a dihedral angle of 22° (Figure 5). Here, the structure is still largely a ketene, but it is beginning to cyclize, with a distance of 2.9 Å between the atoms forming the new bond, and a C=C=O angle of 175°. If the same energy data are plotted versus dihedral angle, it is seen that the energy of the ketene changes little from **TS7a** until an angle of ca. 20°. Then, the energy drops rapidly as rotation continues till the planar oxazinone **15aa** has been formed (Figure S7, Supporting Information). Again, it may be said that, above the inflection point at 22°, the species is essentially the ketene undergoing internal rotation; below this point the ketene is cyclizing to the oxazinone.

1.3-Shift in Ketenes and Ketenimines. Imidoylketenes undergo 1,3-shifts of the substituent on the imine carbon,[10b] in this case an OR group,[12] causing interconversion of ketenes **16** with oxoketenimines **17** (Scheme 2 and Figures 3 and 4). We find that this process has an activation barrier of ca. 28 kcal/mol[13] (from the keten-

(10) (a) Bartsch, R. A.; Chae, Y. M.;Ham, S.; Birney, D. M. *J. Am. Chem. Soc.* **2001**, *123*, 7479−7486. (b) Finnerty, J.; Wentrup, C. *J. Org. Chem.* **2004**, *69*, 1909−1918.

(11) Sheibani, H.; Veedu, R. N.; Wentrup, C. Unpublished results, The University of Queensland, 2003−2004.

(12) Experimental demonstration of 1,3-shifts of OR groups in imidoylketenes and oxoketenimines: (a) Fulloon, B. E.; Wentrup, C. *J. Org. Chem.* **1996**, *61*, 1363−1368. (b) Ramana Rao, V. V.; Wentrup, C. *J. Chem. Soc., Perkin Trans. 1* **1998**, 2583. (c) Wentrup, C.; Ramana Rao, V. V.; Frank, W.; Fulloon, B. E.; Moloney, D. W. J.; Mosandl, T. *J. Org. Chem.* **1999**, *64*, 3608−3619.

(13) This is in line with calculations on other 1,3-shifts of atoms and groups, interconverting oxoketenimines and imidoylketenes: Finnerty, J. J.; Wentrup, C. Unpublished results, The University of Queensland, 2004. See also refs 10b, 14, and 15.

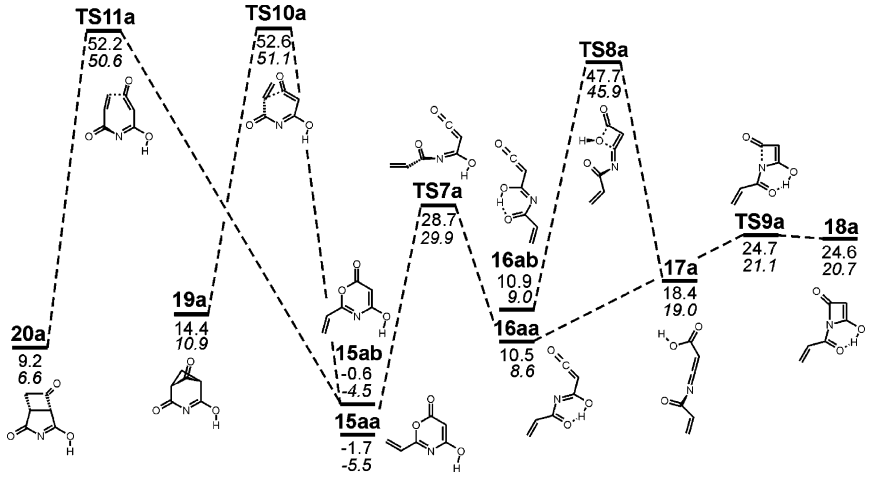

FIGURE 3. Energy profile for oxazine **15a** and ist isomers calculated for the gas phase ($\epsilon = 0$) (roman numbers, B3LYP/6-311+G*//B3LYP/6-31G*; italic numbers, B3LYP/6-31G* energies (kcal/mol)).

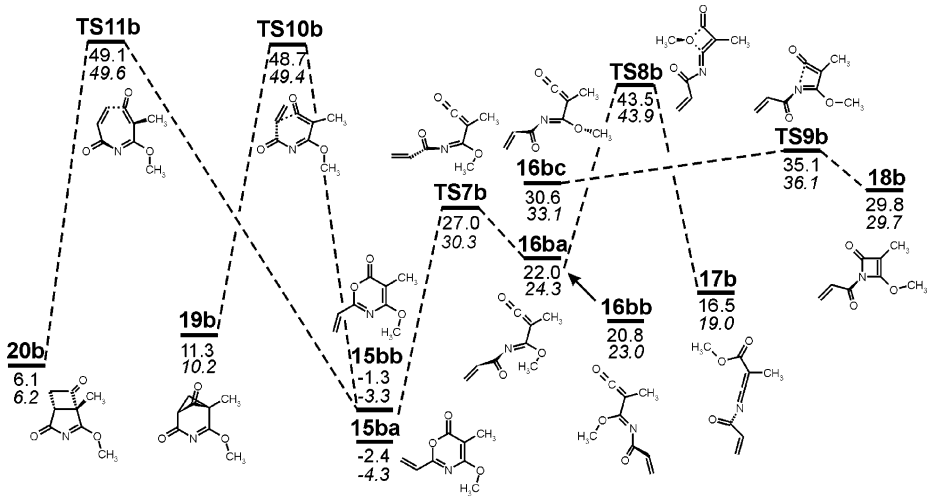

FIGURE 4. Energy profile for oxazine **15b** and ist isomers calculated for the gas phase ($\epsilon = 0$) (roman numbers, B3LYP/6-311+G*//B3LYP/6-31G*; italic numbers, B3LYP/6-31G* energies (kcal/mol)).

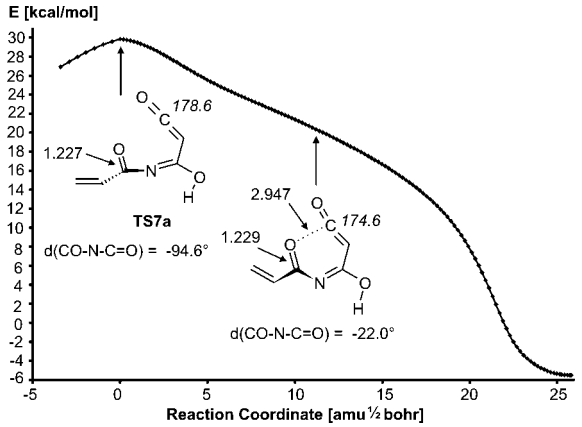

FIGURE 5. Plot of energy vs internal reaction coordinate from **Ts7a** to oxazinone **15a** (B3LYP/6-31G*).

imine side, Figure 3), and the four-membered ring in the transition state **TS8a** is almost planar, as expected for this pseudopericyclic[10b] reaction.

Ketene **16aa** and **16ab** are significantly stabilized relative to the ketenimine **17a** due essentially to an intramolecular O−H−O bond. This is not present in **16b**, thus rendering this ketene less stable than the ketenimine **17b** (Figure 4).

The energy versus internal reaction coordinate graph for the 1,3-shift of OH in ketene **16ab** to ketenimine **17a** via **TS8a** is shown in Figure 6, and a full scale version of this as well as the corresponding graph for the 1,3-OMe shift in ketene **16bb** to ketenimine **17b** via **TS8b** are shown in Figures S8 and S9 (Supporting Information). These curves feature a long "flat" energy profile from about 7 to 20 units on the IRC coordinate (amu$^{1/2}$ bohr). The sharp peak between ca. 3 and −3 IRC units corresponds to the 1,3-shift proper. At an IRC value of 3, the 1,3-shift of OH from **TS8a** to the ketenimine **17a** is almost complete, ((N)C−OH distance 2.17 Å compared to 2.7 Å in **17b**), and the ketenimine function (C=C=N) is fully formed. The dihedral angle between OH and the ketene moiety is still large, as in **TS8a**, but the OH group has now started to rotate and continues to rotate until an IRC value of 5−6 is reached. The *N*-substituent, which was almost in the plane of the four-membered ring in the transition state **TS8a,** now begins to rotate out of that plane to become almost perpendicular in the final

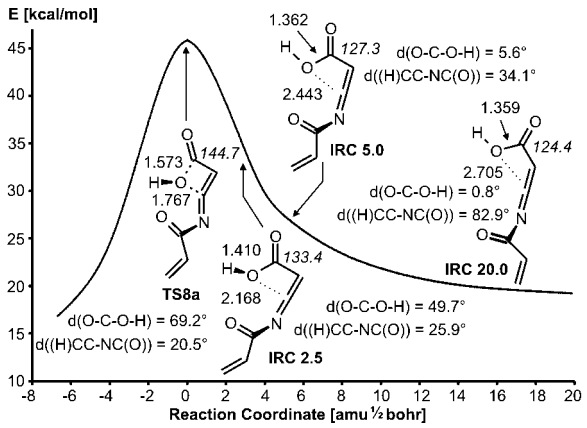

FIGURE 6. Plot of energy vs internal reaction coordinate from ketenimine **17a** (right) via **TS8a** toward ketene **16ab** (left) (B3LYP/6-31G*).

ketenimine product **17a**. Thus, this energy profile can be divided into three (partially) distinct portions: (i) 1,3-shift proper, (ii) rotation of the OH group, and (iii) rotation of the *N*-substituent. The energy vs IRC graph for **TSb8** (Figure S9, Supporting Information) is similar, with a sharp peak for the 1,3-shift proper, but the two rotational motions are more coupled. A similar situation was also found for the 1,3-shifts of NR_2 groups.[10b] All of these 1,3-shifts of donor substituents may be said to be reactions with continuous transition states. The first portion of the activation barrier (coming from the ketenimine side) is due to internal rotation of the donor substituent in order to bring the lone pair into the correct position for overlap with the ketenimine or ketene LUMO. Only the top 10−12 kcal/mol of the barrier is due to the 1,3-shift proper. It is interesting to note that, if the activation energy for the 1,3-shift proper becomes lower than that for rotation, then the 1,3-shift "transition state", **TS8** in this case, would become an *intermediate.* This happens in the α-oxoketene−α-oxoketene rearrangement.[10b,14]

Cyclization to Azetinones. Azetinones are reactive intermediates which in some cases can be observed directly as isomers of imidoylketenes using Ar matrix isolation at cryogenic temperatures.[15] In the present case, cyclization of ketenes **16** to azetinones **18**, 3-azabicyclo-[3.1.1]heptanediones **19** and 3-azabicyclo[3.2.0]heptanediones **20** are considered (Scheme 2 and Figures 3 and 4). The *N*-acylazetinones **18** can be formed from the ketenes **16** with low activation barriers and planar transition states (**TS9**). The *N*-acylazetinones exist in shallow energy minima, which will make their observation difficult. Comparison with the energy profiles for other azetinones[15] indicates that the *N*-acyl groups destabilize the azetinones. The rearrangement of (unobserved) transient *N*-acylazetinones to 1,3-oxazin-6-ones via *N*-acylimidoylketenes has been evaluated as yet another pseudopericyclic reaction with an essentially zero energy barrier for cyclization of the cisoid ketene to the oxazine.[7c] Energy profiles for cyclization of ketene **16aa** to azetinone **18a**, and of **16bc** to azetinone **18b** via **TS9a** and **TS9b**, respectively, are shown in Figures S10 and S11 (Supporting Information).

Cyclization to 3-Azabicyclo[3.1.1]heptanediones and 3-Azabicyclo[3.2.0]heptanediones. Cyclizations of ketenes **16** to 3-azabicyclo[3.1.1]heptanediones **19** and 3-azabicyclo[3.2.0]heptanediones **20** (Scheme 2, Figures 3 and 4) have high activation barriers and will not be competitive among the reactions described in Figure 1 and Figures S1−S4 (Supporting Information). The ketenes **16** are not distinct intermediates on these energy profiles. The energy vs IRC curve for **15a** → **19a** features a long flat portion between −20 to −7 $amu^{1/2}$ bohr (Figure S12, Supporting Information) where the species can be said to be ketene-like, prior to a steep ascent to **TS10**. No intermediates were found between **15** and **19** or between **15** and **20**. Thus, ring opening of **15** plus rotation within the putative ketene and recyclization take place in a smooth, concerted fashion (Figures S12 and S13, Supporting Information).

Conclusion

The facile ring opening of mesoionic 1,3-oxazinium olates **9** to acylketenes **10**, even at room temperature,[1] is corroborated by the calculated activation barriers of less than 20 kcal/mol. The acylketenes **10** are not directly observed because they have energies ca. 10 kcal/mol above the oxazinium olates **9**. The acylketenes **10** recyclize to 3-azabicyclo[3.1.1]heptanetriones **12**.

For the exothermic cyclization of ketenes **10** to oxazinium olates **9** via **TS1** (Scheme 1, Figures 1 and 2) and of ketenes **16** to oxazinones **15** via **TS7** (Scheme 2, Figures 3−5), the major (upper) part of the calculated activation barrier is due to rotation within the ketene, and only the minor (lower) part is due to the actual cyclization process, the latter leading to a planar structure and being pseudopericyclic in nature. The cyclizations of ketenes **11** to oxazinium olates **9** via **TS4** also follow computationally concerted paths (Scheme 1, Figure S14 (Supporting Information)), as do the computationally concerted ring opening plus rotation plus recyclization reactions **15** → **19** and **20** via **TS10** and **TS11**, respectively (Scheme 2, Figures 3 and 4, and Figures S12 and S13 (Supporting Information0). For the 1,3-shifts of the OR group that interconvert ketenes **16** and ketenimines **17** via four-membered cyclic transition states **TS8** (Figure 9 and Figures S8 and S9 (Supporting Information)) the first portion (from the ketenimine side) of the activation barrier is due largely to internal rotation of substituents and the top part is due to the 1,3-shift proper.

Acknowledgment. This work was supported by the Australian Research Council and by the APAC National Facility Merit Allocation Scheme (computing).

Supporting Information Available: Figures S1−S4 showing the energy profiles for **9a**−**d** analogous to Figure 1, Figures S5 and S6 showing the calculated IR spectra of compounds **9a**−**d** for $\epsilon = 0$ and 40, Figure S7 analogous to Figure S8 but with dihedral angle as abscissa, and Figures S8−S14 being graphs of energy vs internal reaction coordinate around **TS8**−**TS11** and **TS4b**. Tables S1−S6 of calculated relative energies (+ZPE) of ground and transition states and imaginary frequencies of the latter for all compounds in Figures 1−6 and Chart 1. Cartesian coordinates, absolute energies, and relevant frequencies of calculated compounds. This material is available free of charge via the Internet at http://pubs.acs.org.

JO050429E

(14) Wong, M. W.; Wentrup, C. *J. Org. Chem.* **1994**, *59*, 5279−5285.
(15) George, L.; Netsch, K.-P.; Bernhardt, P. V.; Wentrup, C. *Org. Biomol. Chem.* **2004**, *2*, 3518−3523.